Supporting Information

Balancing the Electrical Double Layer Capacitance and Pseudocapacitance of Hetero-atom Doped Carbon

Zi-Hang Huang [a,b]‡, Tianyu Liu[b]‡, Yu Song[a,b], Yat Li[b]* and Xiao-Xia Liu[a]*

[a] Department of Chemistry, Northeastern University, Shenyang, 110819, China

[b] Department of Chemistry and Biochemistry, University of California, 1156 High Street, Santa Cruz, California, 95064, United States

* Corresponding authors: Xiao-Xia Liu, xxliu@mail.neu.edu.cn; Yat Li, yatli@ucsc.edu

‡ These authors contributed equally to this work.

1. Calculations

1.1 Capacitances of single electrode

The areal and gravimetric capacitance of a single electrode can be calculated based on galvanostatic charge-discharge experiments according to Equation S1 and S2:

$$C_s = \frac{I \times t}{\Delta U \times S} \quad \text{(Equation S1)}$$

$$C_m = \frac{I \times t}{\Delta U \times m} \quad \text{(Equation S2)}$$

Where C_s and C_m (mF/cm^2 or F/g) are the areal and gravimetric capacitance, I the discharge current (mA), t the time (s), ΔU the potential window (V), S the working area of electrode (cm^2), m is the mass of active material (NOC or MnO_2). The mass loadings of all NOC electrodes were controlled to be 2.3 mg/cm^2 by adjusting the electro-deposition time. The mass loading of MnO_2 NSAs is 1.0 mg/cm^2.

1.2 Capacitances of NOC//MnO_2 Devices

The volumetric capacitance (C_v, unit in F/cm^3) of NOC//MnO_2 can be calculated based on galvanostatic charge-discharge experiments according to Equation S3:

$$C_V = \frac{I \times t}{\Delta U \times V} \quad \text{(Equation S3)}$$

Where I is the charge-discharge current (A), t the discharge time (s), ΔU the potential window (V) and V the total volume (cm^3) of the whole device stack including two electrodes, electrolyte-soaked separator and packages. The working area and thickness of the NOC//MnO_2 device are *ca.*1 cm^2 and 0.0735 cm, respectively. The whole volume of the NOC//MnO_2 device are about 0.0735 cm^3 [1 cm (L) × 1 cm (W) × 0.0735 cm (H)].

The gravimetric capacitance of ASC device can be calculated based on galvanostatic charge-discharge experiments according to Equation S4:

$$C_m = \frac{I \times t}{\Delta U \times m} \quad \text{(Equation S4)}$$

where C_m (F/g) is the gravimetric capacitance. I is the discharge current (mA). t is the discharge time (s). ΔU is the potential window (V). m is the mass of active material (mg).

1.3 Energy density and power density of NOC//MnO_2 Devices

Volumetric energy density (E, Wh/cm^3) and volumetric power density (P, W/cm^3) are calculated using the following two equations:

$$E_V = \frac{C_V \times \Delta U^2}{2 \times 3600} \quad \text{(Equation S5)}$$

$$E_V = \frac{3600 \times E}{t} \quad \text{(Equation S6)}$$

Where C_v (F/cm^3) is the specific capacitance, ΔU the potential window (V) and t the discharge time (s).

Gravimetric energy density (E, Wh/kg) and power density (P, W/kg) are calculated using the following two equations:

$$E_m = \frac{1000 \times C_m \times \Delta U^2}{2 \times 3600} \quad \text{(Equation S7)}$$

$$P_m = \frac{3600 \times E_m}{t} \quad \text{(Equation S8)}$$

where C_m (F/g) is the specific capacitance of ASC device, ΔU is the potential window (V) and t is the discharge time (s).

1.4 Charge balance for NOC//MnO_2 Devices

To achieve the maximum and stable performance of the ASC device, the capacity (Q) of negative and positive electrode should be balanced, *i.e.*,

$$Q_+ = Q_- \quad \text{(Equation S9)}$$

The capacity is associated with areal capacitance (C_s), potential window (ΔU) and working area of electrode (S), as shown in Equation S10:

$$Q = C_s \times \Delta U \times S \quad \text{(Equation S10)}$$

Combining Equation S9 and S10, the areal ratio of negative electrode to positive electrode should satisfy Equation S11:

$$\frac{S_-}{S_+} = \frac{(C_{S,+}) \times (\Delta U_+)}{(C_{S,-}) \times (\Delta U_-)} \quad \text{(Equation S11)}$$

Substitute $C_{s,+}$=356.4 mF/cm^2 (@ 1 mA/cm^2), $C_{s,-}$=324 mF/cm^2 (@ 1 mA/cm^2), ΔU_-= 1.1 V and ΔU_+= 1.0 V, the areal ratio is about 1. In our work, we fixed the working area of both electrodes to be 1.0 cm^2.

2. Supplementary Figures and Tables

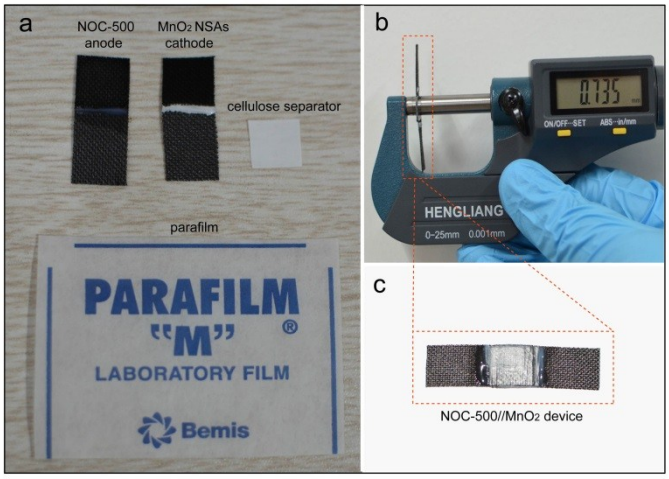

Figure S1. Digital photographs of ASC devices' components include NOC-500 anode, MnO_2 NSAs cathode, a piece of cellulose separator and parafilm (a). Photograph of thickness measurements process (b, c).

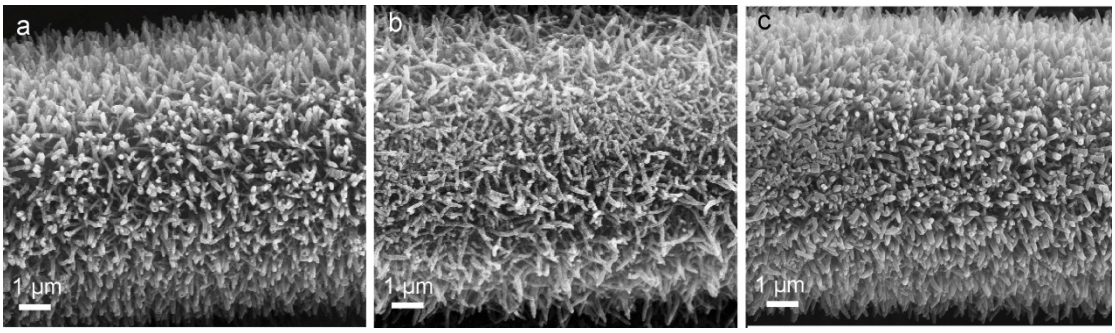

Figure S2. SEM images of (a) NOC-400, (b) NOC-500 and (c) NOC-600.

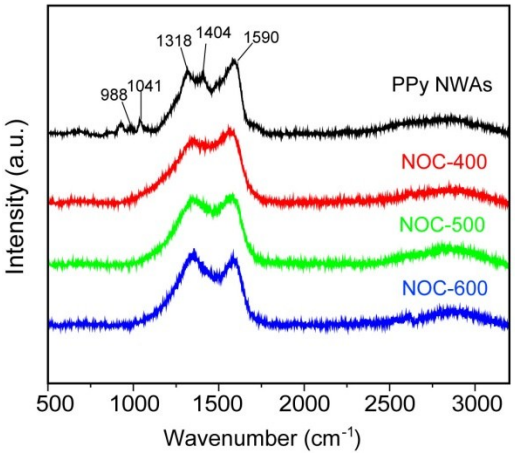

Wavenumber (cm^{-1})	assignment [1,2]
998	Ring deformation
1041	In-plane C-H bending
1318	Anti-symmetrical C-N stretching
1404	Anti-symmetrical C-N stretching
1590	C=C stretching

Figure S3. Raman spectra of PPy NWAs, and all NOC samples (a). The tables show the assignments for the major peaks in the spectra.

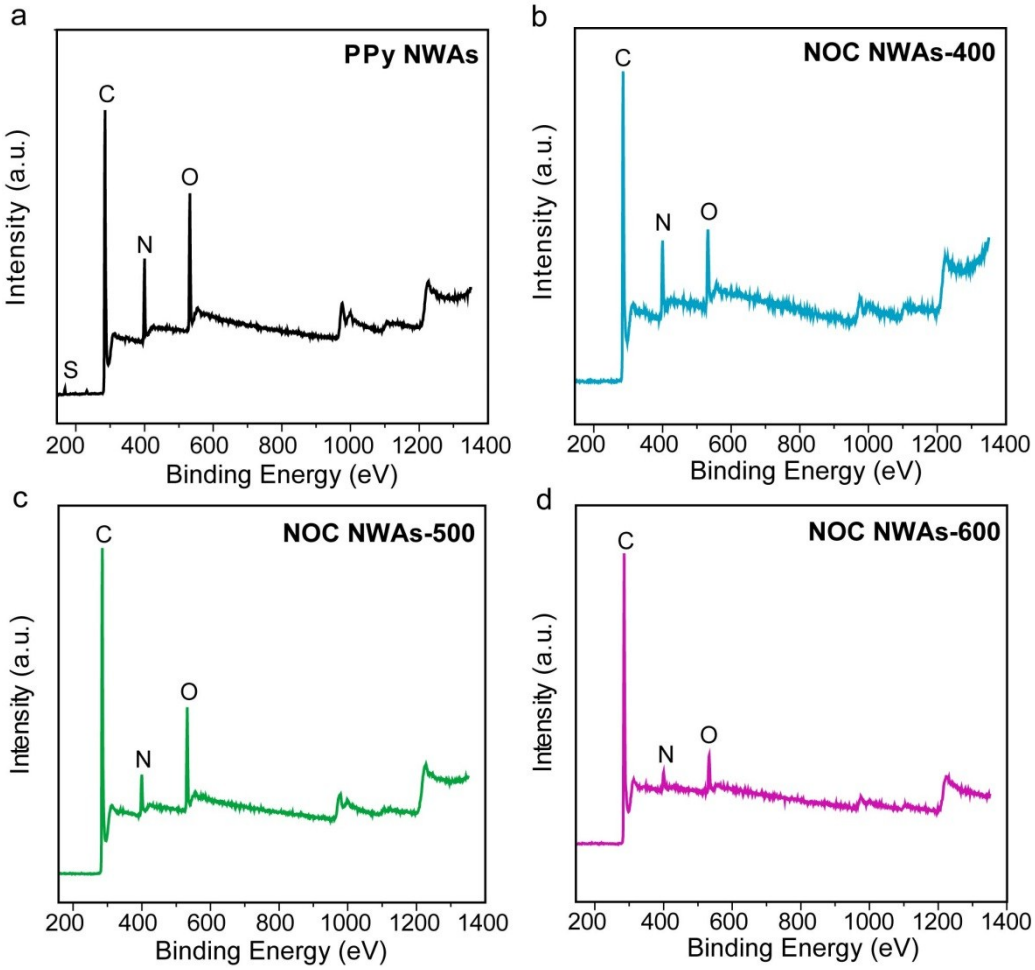

Figure S4. XPS survey spectra collected for (a) PPy NWAs, (b) NOC-400, (c) NOC-500 and (d) NOC-600.

Table S1 Summary of the atomic percentage and electrochemical performances of prepared samples

Sample Name	Element composition (at.%)		Combined series resistance (ohm)	Capacitance	
	N	O		@ 1 mA/cm^2	@ 100 mA/cm^2
PPy	11.97	14.40	1.39	526 mF/cm^2 (228 F/g @0.43A/g)	2.63 mF/cm^2 (1.14 F/g @43.5A/g)
NOC-400	9.87	12.03	1.36	434 mF/cm^2 (188 F/g @0.43A/g)	108 mF/cm^2 (47 F/g @43.5A/g)
NOC-500	7.95	11.29	0.96	324 mF/cm^2 (141 F/g @0.43A/g)	184.7 mF/cm^2 (80.3 F/g @43.5A/g)
NOC-600	5.50	6.45	0.91	229 mF/cm^2 (99.6 F/g @0.43A/g)	139 mF/cm^2 (60.5 F/g @43.5A/g)

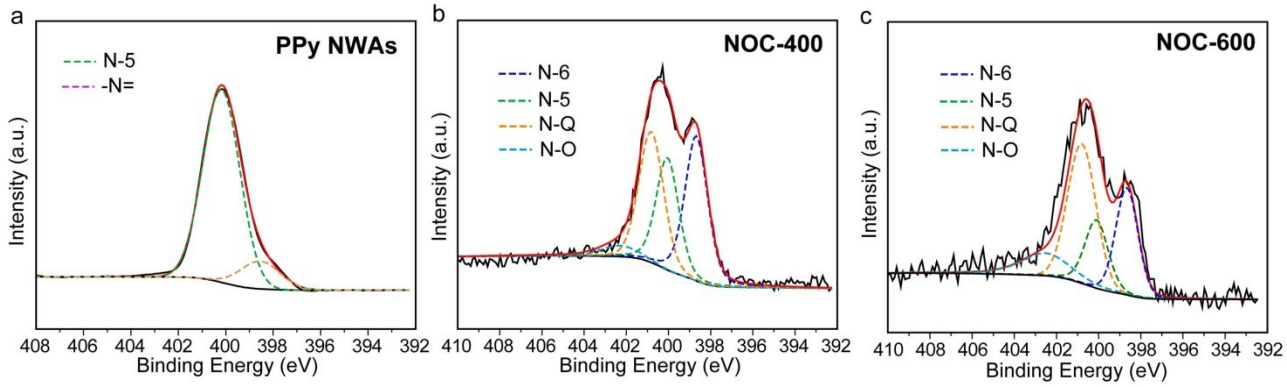

Figure S5. High resolution N 1s XPS peak of (a) PPy NWAs, (b) NOC-400 and (c) NOC-600. The solid black curves are experimental data. The dashed lines are synthetic peaks and the solid red lines are the sums of all synthetic peaks.

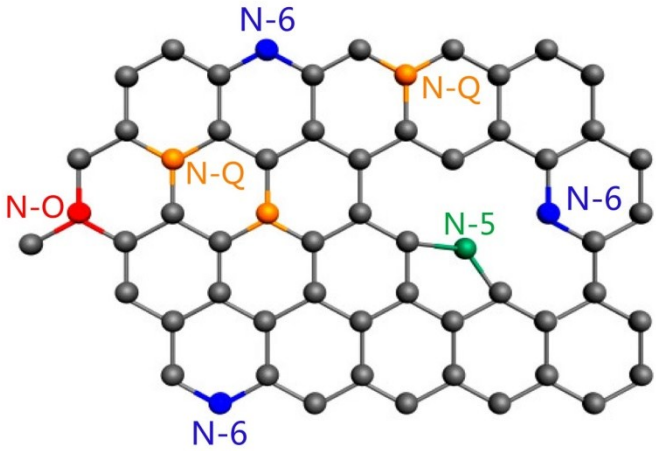

Figure S6. Schematic illustration showing different N-functionalities: pyrrolic nitrogen (N-5), pyridinic nitrogen (N-6), quaternary nitrogen (N-Q), and oxidized nitrogen (N-O).

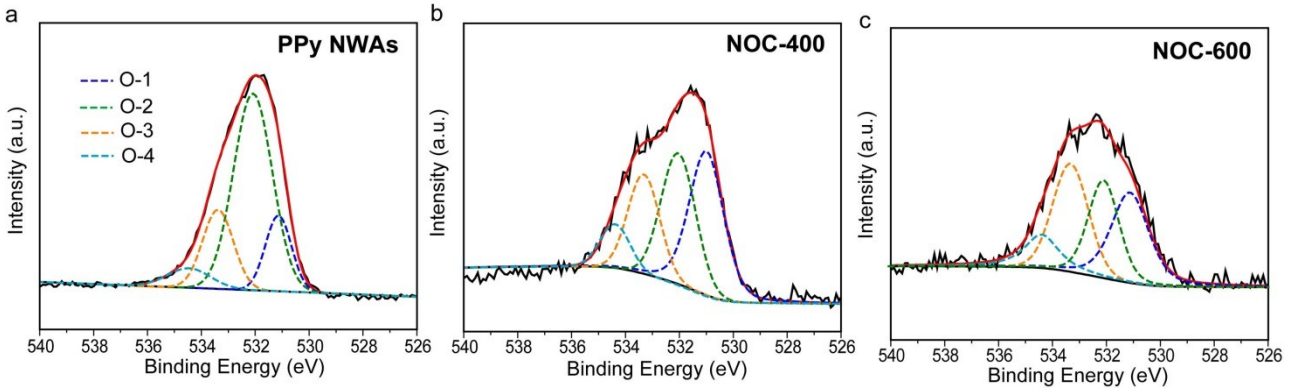

Figure S7. High resolution O 1s XPS peak of (a) PPy NWAs, (b) NOC-400 and (c) NOC-600. The solid black curves are experimental data. The dashed lines are synthetic peaks and the solid red lines are the sums of all synthetic peaks.

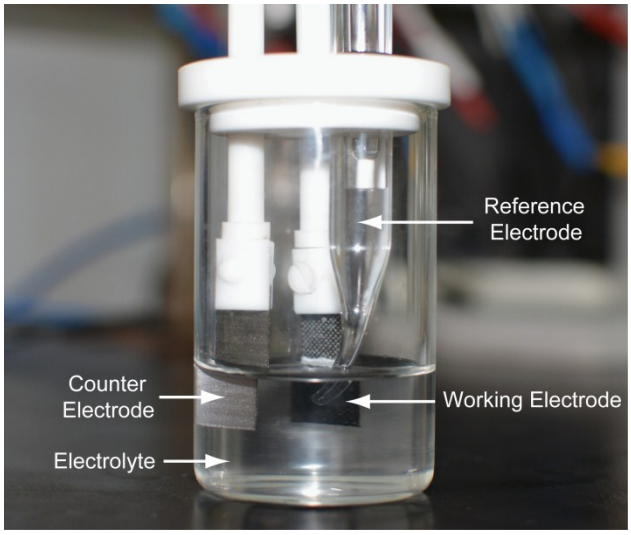

Figure S8. A digital picture of the three-electrode electrolytic cell used for electrochemical tests.

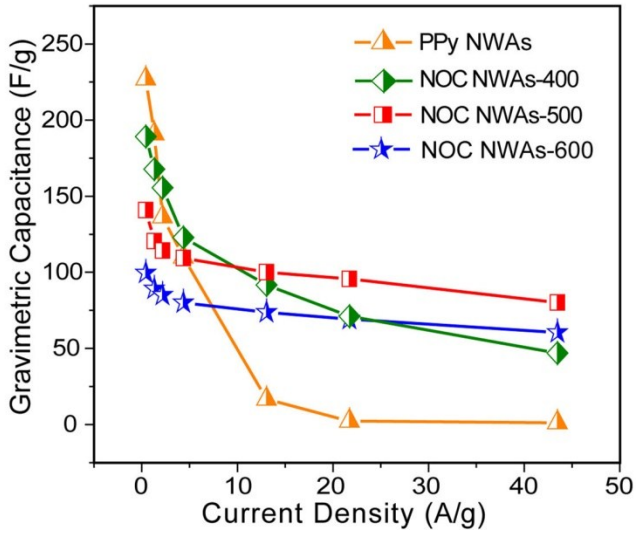

Figure S9. Gravimetric capacitance of all NOC and PPy electrodes collected at different scan rates.

Among all the NOC electrodes and the PPy electrode, NOC-500 exhibited the highest gravimetric capacitance of 80.3 F/g at 43.5 A/g with a rate capability of 57% (from 0.43 A/g to 43.5 A/g). This trend is in agreement with the areal capacitance.

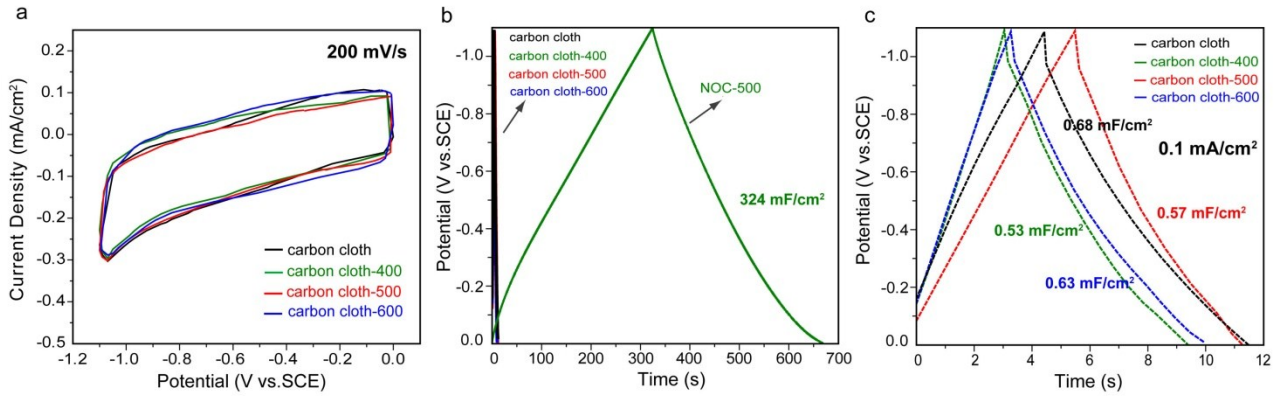

Figure S10. Electrochemical performance of carbon cloth substrates in 5 M LiCl aqueous electrolyte. (a) Cyclic voltammograms collected for carbon cloth samples treated at different temperatures (scan rate: 200 mV/s). (b) Comparison of the GCD profile of NOC-500 (1 mA/cm^2) and the GCD profiles of various carbon substrates (0.1 mA/cm^2). (c) GCD profiles of various carbon cloth samples.

Trasatti Method Analysis

Trasatti method is used to evaluate capacitive contribution from electrical double layer and pseudo-capacitive reactions. The main steps involving the analysis are as follows:

1. Data collection

Collect cyclic voltammograms at different scan rates and evaluate corresponding areal capacitances based on the following equation:

$$C = \frac{S}{2 \cdot \Delta U \cdot v} \quad (Equation\ S12)$$

where C is the areal capacitance (in mF/cm^2), ΔU the potential window (in V), S the area enclosed by corresponding cyclic voltammograms (in mA·V/cm^2) and v the scan rate (in V/s).

2. Evaluation of maximum capacitance (C_T)

Assuming ion diffusion follows a semi-infinite diffusion pattern (*i.e.*, ions unrestrictedly diffuse to electrode/electrolyte interface from bulk electrolyte), a linear correlation between the reciprocal of the calculated areal capacitance (C^{-1}) and the square root of scan rates ($v^{1/2}$) should be observed[3]:

$$C^{-1} = constant \cdot v^{1/2} + {C_T}^{-1} \quad \text{(Equation S13)}$$

where C, v and C_T represent calculated areal capacitance, scan rate and maximum areal capacitance, respectively. The "maximum capacitance (C_T)" is treated as the sum of electrical double layer capacitance and pseudo-capacitance.[4] C_T equals the reciprocal of the y-intercept of the C^{-1} vs. $v^{1/2}$ plot (Figure S10, left columns).

3. Evaluation of maximum electrical double layer capacitance and maximum pseudo-capacitance

Plotting the calculated areal capacitances (C) against the reciprocal of square root of scan rates ($v^{-1/2}$) should also give a linear correlation described by the following equation (assuming a semi-infinite diffusion pattern)[5]: (Figure S10, right columns)

$$C = constant \cdot v^{-1/2} + C_{EDL} \quad \text{(Equation S14)}$$

where C, v and C_{EDL} is the calculated areal capacitance, scan rate and maximum electrical double layer capacitance, respectively. Linear fit the plot and extrapolate the fitting line to y-axis gives the C_{EDL}.[4] Subtraction of C_{EDL} from C_T yields the maximum pseudo-capacitance (C_{PS}).

4. Evaluation of the percentage of capacitance contribution

The capacitance contribution can be evaluated based on the following equation:

$$C_{EDL}\% = \frac{C_{EDL}}{C_T} \times 100\% \quad \text{(Equation S15)}$$

$$C_{PS}\% = \frac{C_{PS}}{C_T} \times 100\% \quad \text{(Equation S16)}$$

where C_{EDL}% and C_{PS}% stand for capacitance percentage of electrical double layer capacitance and pseudo-capacitance.

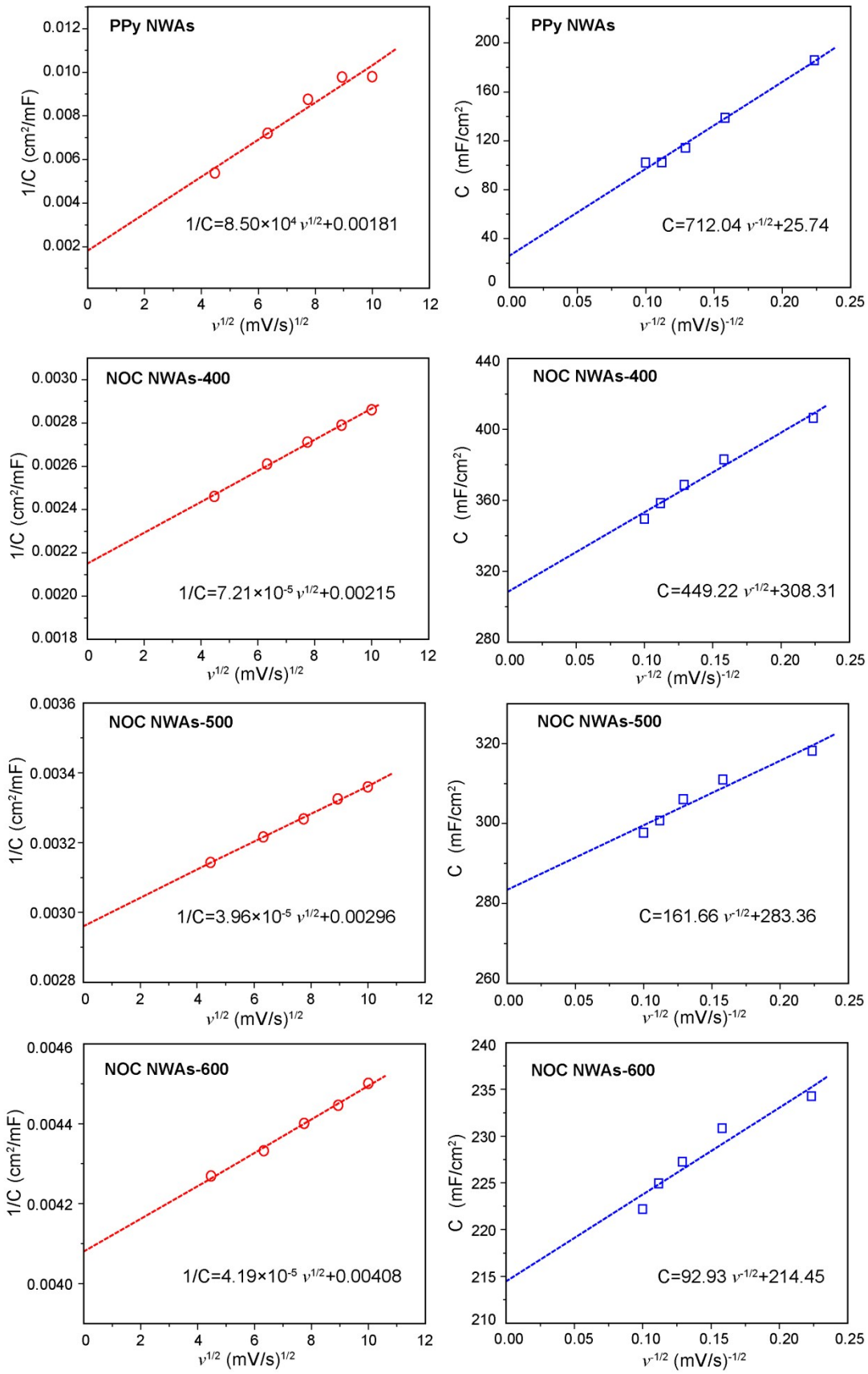

Figure S11. Left column: plots of reciprocal of areal capacitance (C^{-1}) *vs.* square root of scan rate ($v^{1/2}$). Right column: plots of gravimetric capacitance (C) *vs.* reciprocal of square root of scan rate ($v^{-1/2}$). The solid lines are linear fitting lines of data points. The algebraic equations of the fitting

lines are shown in the inset. (a) PPy NWAs, (b) NOC-400, (c) NOC-500, and (d) NOC-600.

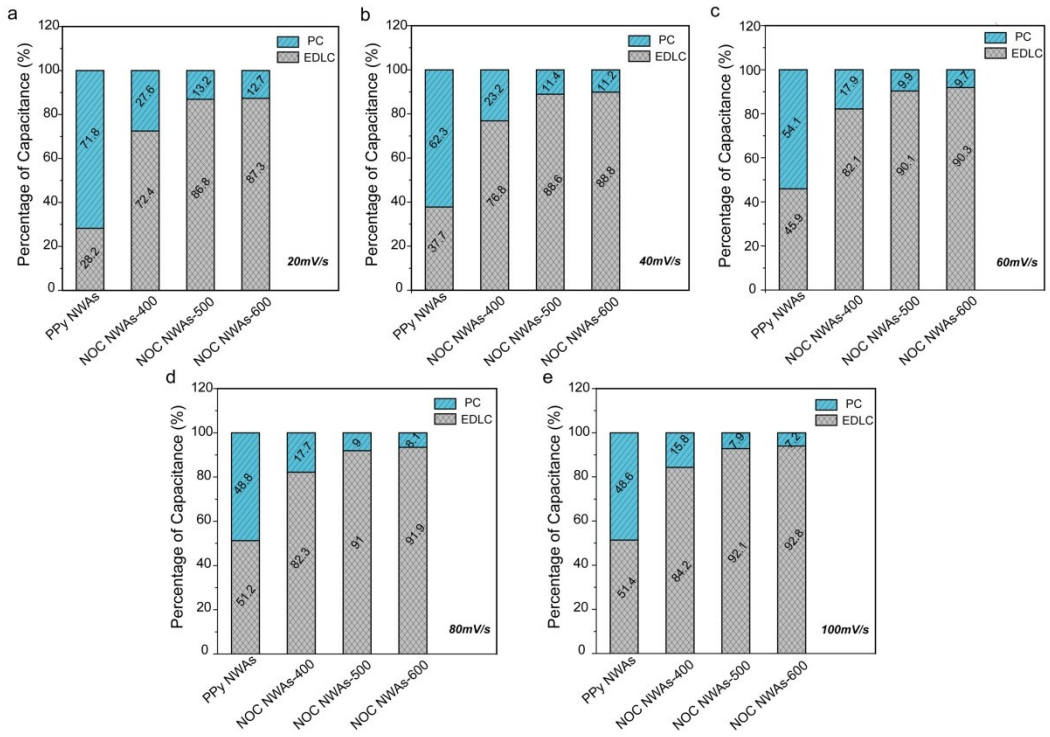

Figure S12. Percentage of capacitance contribution evaluated for PPy and all NOC samples under different scan rates.

The details about the capacitance differentiation can be found in the previously reported work.[5]

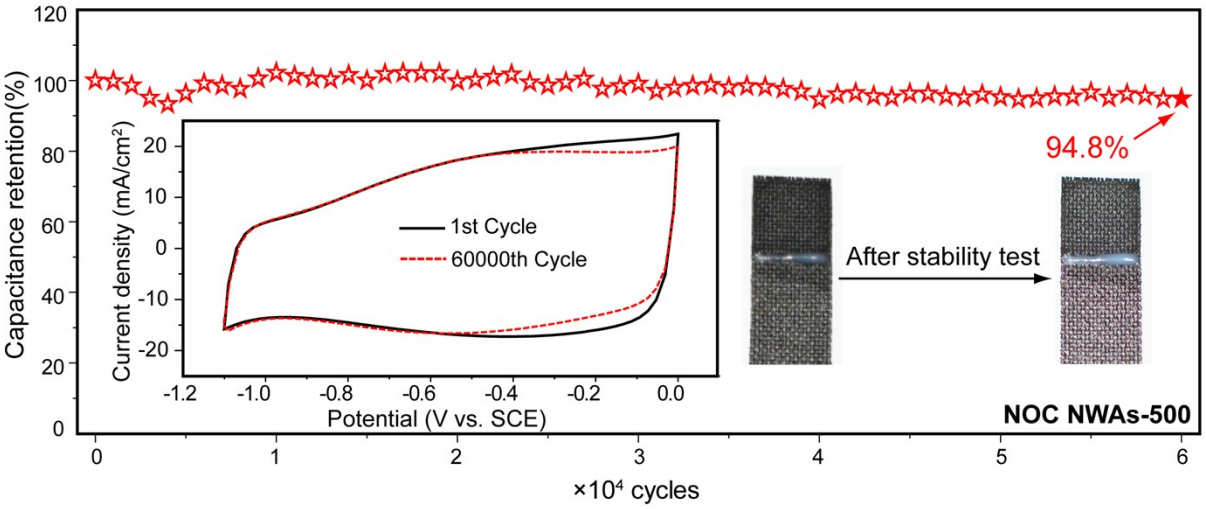

Figure S13. Cycling stability of NOC-500 evaluated by cyclic voltammetry at 50 mV/s in 5 M LiCl aqueous electrolyte. Inset compares the CVs collected at the first and last cycle and the electrode before and after the cycling stability test.

Characterizations of manganese dioxide nanosheet arrays (MnO_2 NSAs)

Figure S14a-c show the morphology of the as-prepared MnO_2 NSAs. It can be seen that MnO_2 clusters were uniformly deposited on carbon fibers. Close examination reveals that each cluster is consisted of a number of vertically aligned MnO_2 nanosheets interconnected with each other (Figure S14c). The highly open and porous 3D architecture is beneficial for fast ion diffusion. Figure S14d shows a representative TEM image of several MnO_2 nanosheets. The thickness of nanosheet is around 10-15 nm and the selected area electron diffraction (SAED) pattern (Figure S14d inset) confirms that the armorphous nature of the as-deposited MnO_2 nanosheets.

To determine the chemical composition of the deposited NSAs, XPS spectra was collected. The survey spectrum (Figure S15a) contains signals from Mn, C and O elements in the electrode which indicates manganese oxide is successfully deposited on carbon fibers. To further investigate the valence state of Mn, the high resolution Mn 2p peak and Mn 3s peak are de-convoluted. In the Mn 2p spectrum (Figure S15b), there are two synthetic peaks located at 654.3 and 642.4 eV, which can be assigned to Mn $2p_{1/2}$ and Mn $2p_{3/2}$ spin-orbit peaks of MnO_2, respectively.[6] The energy separation of the two peaks from Mn 3s (Figure S15c) is measured to be 4.57 eV, a characteristic value of Mn^{4+} ions.[7-9] Taking together, we are confident that the chemical composition of the deposited NSAs is MnO_2.

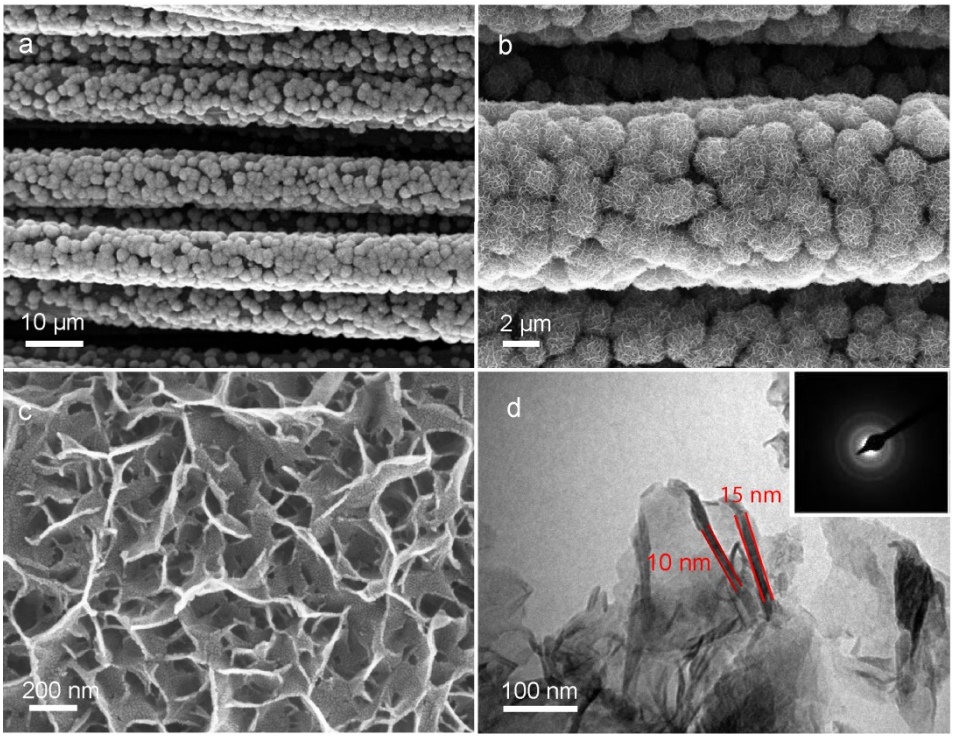

Figure S14. (a-c) The SEM images and (d) the TEM image of MnO_2 NSAs. Inset of (d) shows the SAED image.

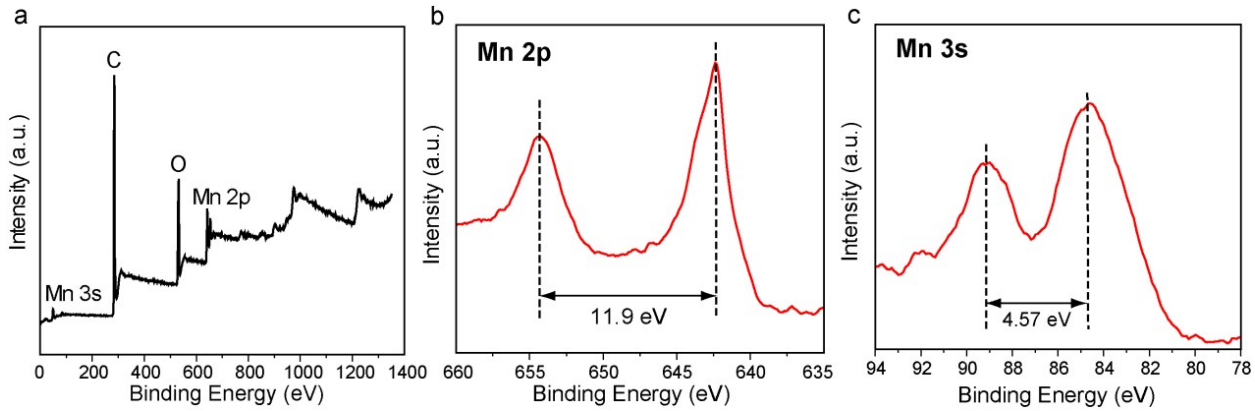

Figure S15. (a) XPS survey spectrum of MnO_2 NSAs. High resolution (b) Mn 2p and (c) Mn 3s XPS peak. Peak separations are highlighted and labelled.

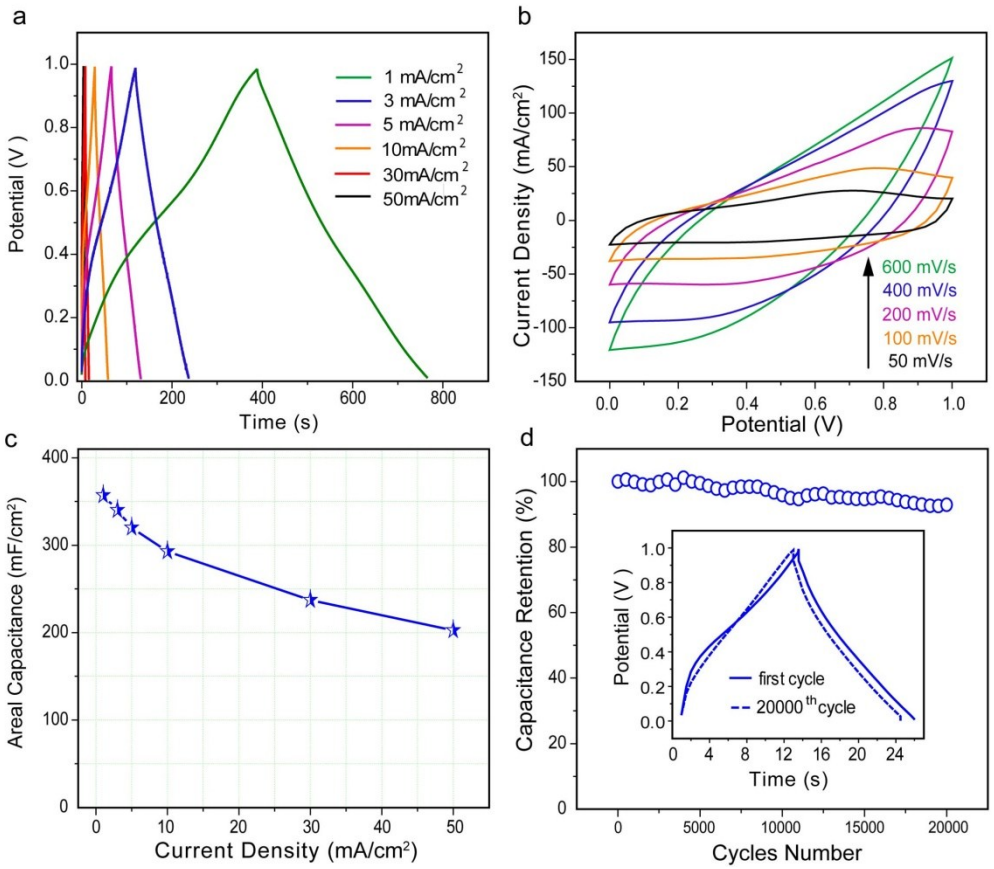

Figure S16. Electrochemical performance of the MnO_2 NSAs tested in 5 M LiCl aqueous electrolyte. (a) GCD profiles collected at various current densities. (b) CVs measured at different scan rates in a three-electrode cell. (c) Plot of areal capacitance vs. various current densities. Capacitances are calculated based on GCD profiles. (d) Cycling stability with the inset shows the

GCD profiles collected in the first and the last cycle.

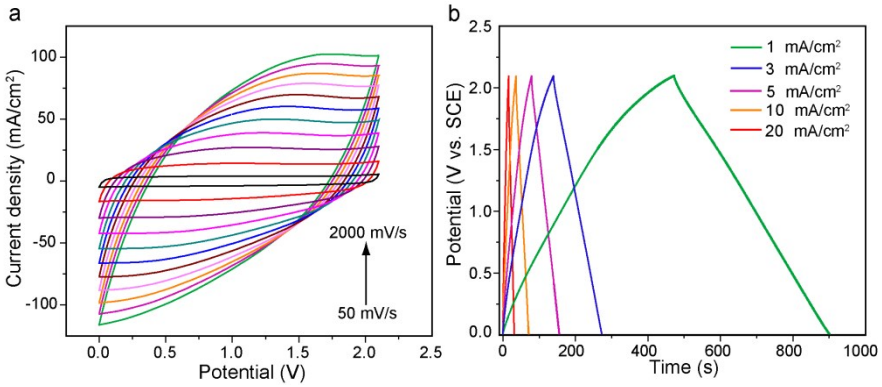

Figure S17. Electrochemical performance of the NOC-500//MnO_2 ASC. (a) CVs measured at various large scan rates and (b) GCD profiles collected at various current densities.

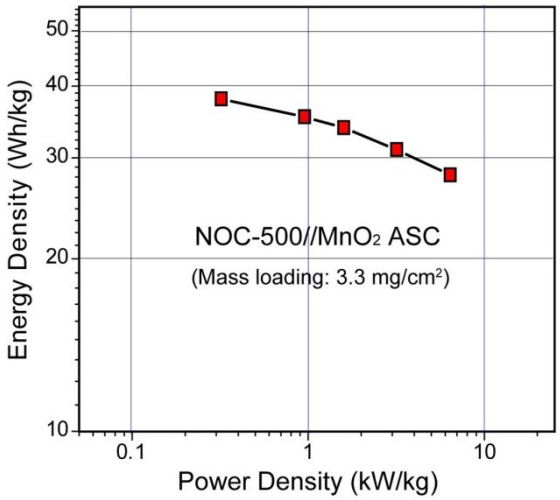

Figure S18. The gravimetric energy density and power density of the NOC-500//MnO_2 ASC.

References

1 M. Li, Z. Wei, L. Jiang, *J. Mater. Chem.* 2008, **18**, 2276-2280.

2 Lindfors, T.; Kvarnstrom, C.; Ivaska, A. J. Electroanal. Chem. 2002, **2**, 131-138.

3 S. Ardizzone, G. Fregonara, S. Trasatti, *Electrochim. Acta* 1990, **35**, 263.

4 Y. H. Lee, K. H. Chang, C. C. Hu, *J. Power Sources* 2013, **227**, 300.

5 J. Duay, S. Sherrill, Z. Gui, E. Gillette, S. B. Lee, *ACS Nano* 2013**, 7,** 1200.

6 L. H. Du, P. H. Yang, X. Yu, P. Y. Liu, J. H. Song, W. J. Mai, *J. Mater. Chem.A* 2014, **2**, 17561.

7 Z. B. Lei, Z. T. Zhang, X. S. Zhao, *J. Mater. Chem.* 2012, **22**, 153.

8 M. Toupin, T. Brousse, D. Belanger, *Chem. Mater.* 2004, **16**, 3184.

9 M. Toupin, T. Brousse, D. Belanger, *Chem. Mater.* 2002, **14**, 3946.